*Electronic Supplementary Information*

# Micromotor-Assisted Highly Efficient Fenton Catalysis by Laccase/Fe-BTC-$NiFe_2O_4$ Nanozyme Hybrid with 3D Hierarchical Structure

Jie Yang[a], Jia Li[*a], Dickon H. L. Ng[b, c], Ping Yang[*a], Wenning Yang[a], Yong Liu[a]

[a] *School of Material Science and Engineering, University of Jinan, Jinan, 250002, P. R. China*

[b] *Department of Physics, The Chinese University of Hong Kong, Shatin, Hong Kong, 999077, P. R. China*

[c] *Key Laboratory of Materials Processing & Mold, Ministry of Education, Zhengzhou University, Zhengzhou, 450000, P. R. China*

**Email: mse_lij@ujn.edu.cn; mse_pingy@ujn.edu.cn*

## Table of Content

**Section 1: Supporting Video**

**Video S1**. The video of the moving laccase@Fe-BTC/$NiFe_2O_4$-MT in 0.5%, 1%, 3%, 5% $H_2O_2$ solution containing 0.5 % of sodium dodecyl sulfonate.

**Section 2: Figures**

**Fig. S1**. XPS spectra of laccase@Fe-BTC/$NiFe_2O_4$-MT: survey (a), C1s (b), O1s (c), Fe2p (d), Mn2p (e), Ni (f), S (g), N (h) and Cu (i).

**Fig. S2**. SEM images of laccase@Fe-BTC/$NiFe_2O_4$-MT-X. X represented the mass ratio of $FeCl_3 \cdot 6H_2O$: $NiFe_2O_4$-MT in the process of synthesis. laccase@Fe-BTC/$NiFe_2O_4$-MT-0.1 (a-c), laccase@Fe-BTC/$NiFe_2O_4$-MT-0.2 (d-f), laccase@Fe-BTC/$NiFe_2O_4$-MT-1 (g-i) and laccase@Fe-BTC/$NiFe_2O_4$-MT-2 (j-l).

**Fig. S3**. Photographs of laccase@Fe-BTC/$NiFe_2O_4$-MT with and without external magnetic field.

**Fig. S4.** Effect of the initial concentration of laccase solution used in the synthesis process on the laccase loading.

**Fig. S5.** Percentage laccase leaching along the time for laccase@Fe-BTC and laccase@Fe-BTC/$NiFe_2O_4$-MT.

**Fig. S6.** The decolorization of MB in terms of TOC removal.

**Fig.S7**. The pore distributions of samples (pore diameter between 2nm and 10 nm).

## Section 3: Tables

**Table. S1**. Pore texture parameters of the as-synthesized samples

**Table. S2**. Movement rate, drag force and work efficiency of $NiFe_2O_4$-MT

**Table. S3.** Movement rate, drag force and work efficiency of laccase@Fe-BTC/$NiFe_2O_4$-MT

## Section 4: The description of physical parameters, Bradford analyses and leaching test

## Section 2: Figures

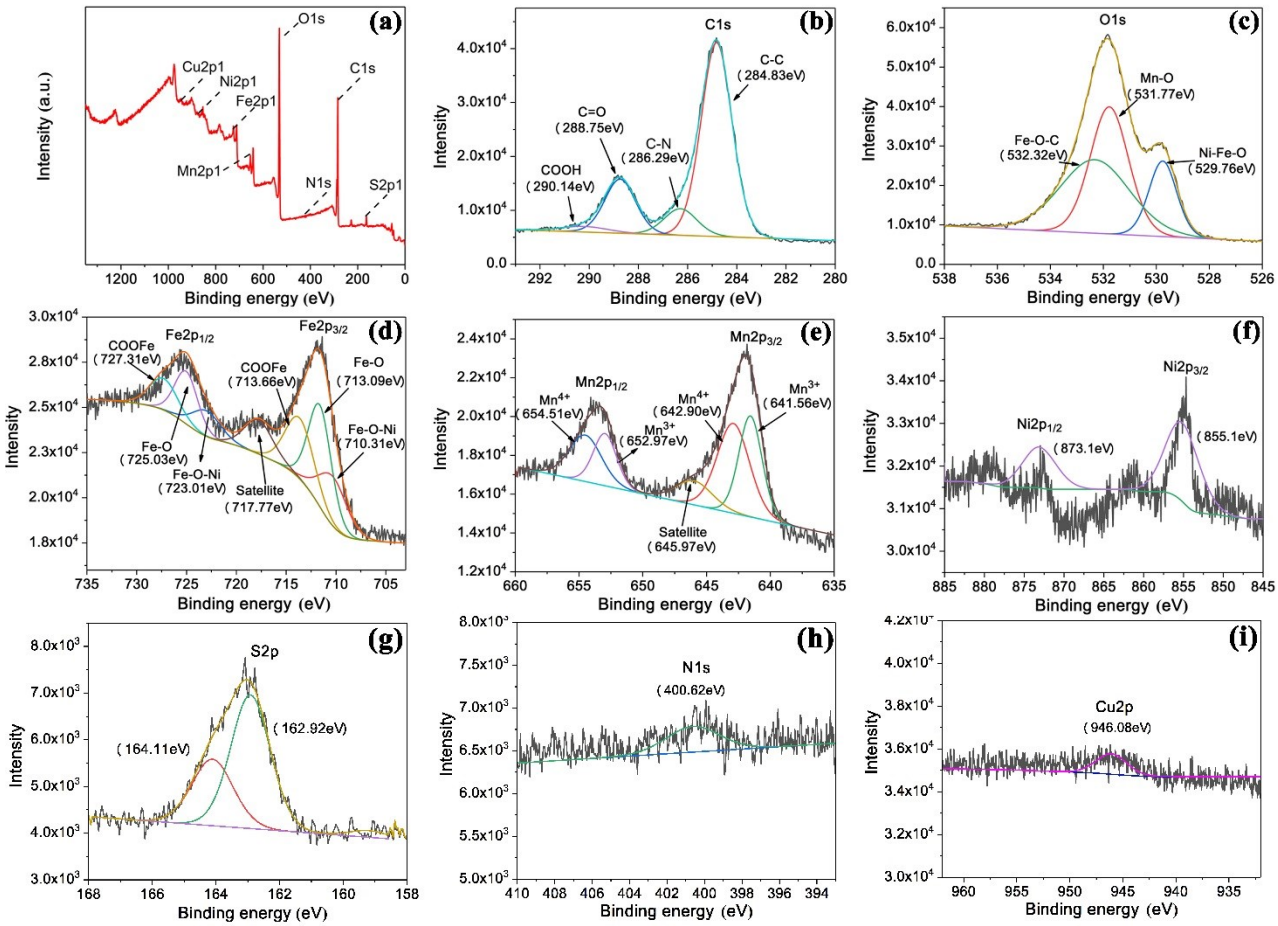


**Fig. S1.** XPS spectra of laccase@Fe-BTC/$NiFe_2O_4$-MT

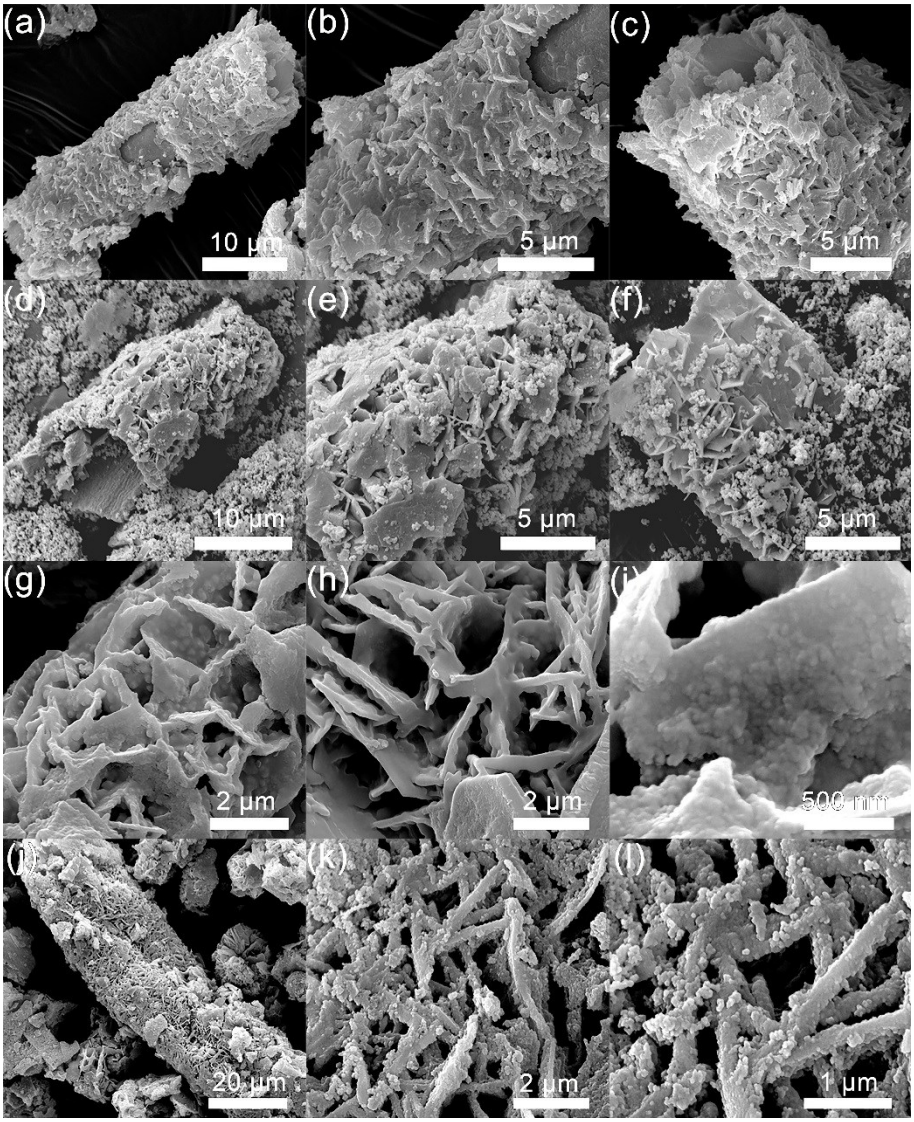


**Fig. S2.** FESEM images of laccase@Fe-BTC/$NiFe_2O_4$-MT-0.1 (a-c), laccase@Fe-BTC/$NiFe_2O_4$-MT-0.2 (d-f), laccase@Fe-BTC/$NiFe_2O_4$-MT-1 (g-i) and laccase@Fe-BTC/$NiFe_2O_4$-MT-2 (j-l).

**Fig. S3**. Photographs of laccase@Fe-BTC/$NiFe_2O_4$-MT with and without external magnetic field

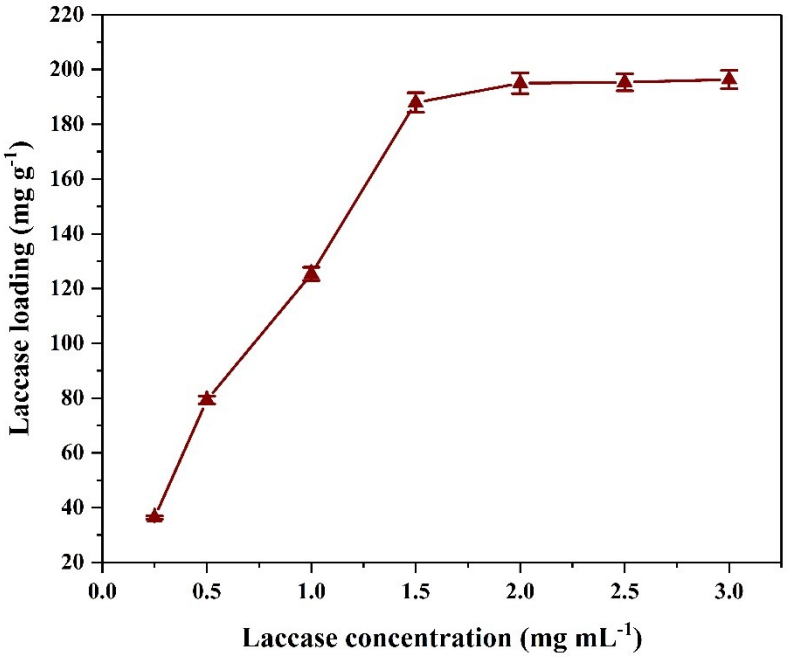


**Fig. S4. Effect of the initial concentration of laccase solution used in the synthesis process on the laccase loading.**

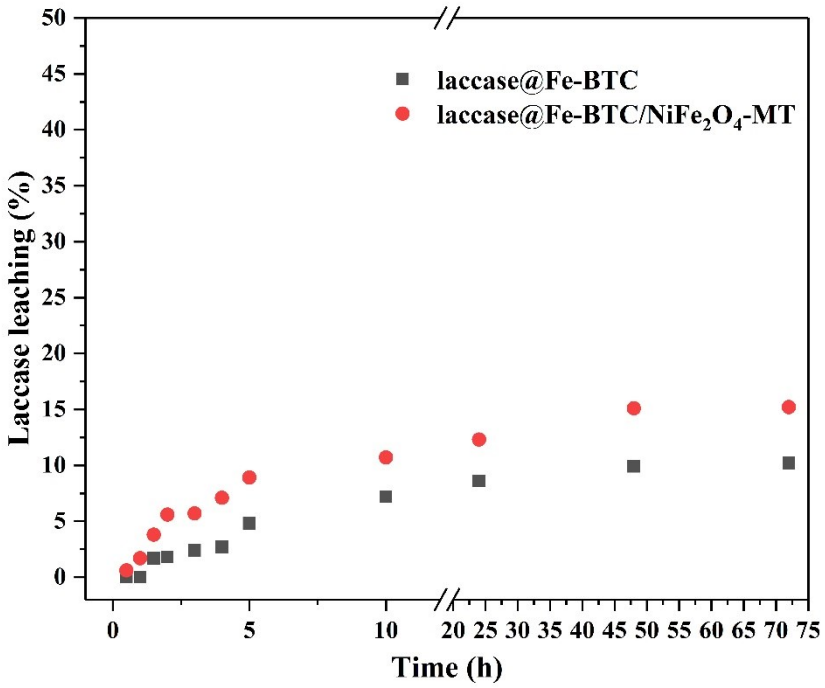


**Fig. S5. Percentage laccase leaching along the time for laccase@Fe-BTC and laccase@Fe-BTC/$NiFe_2O_4$-MT.**

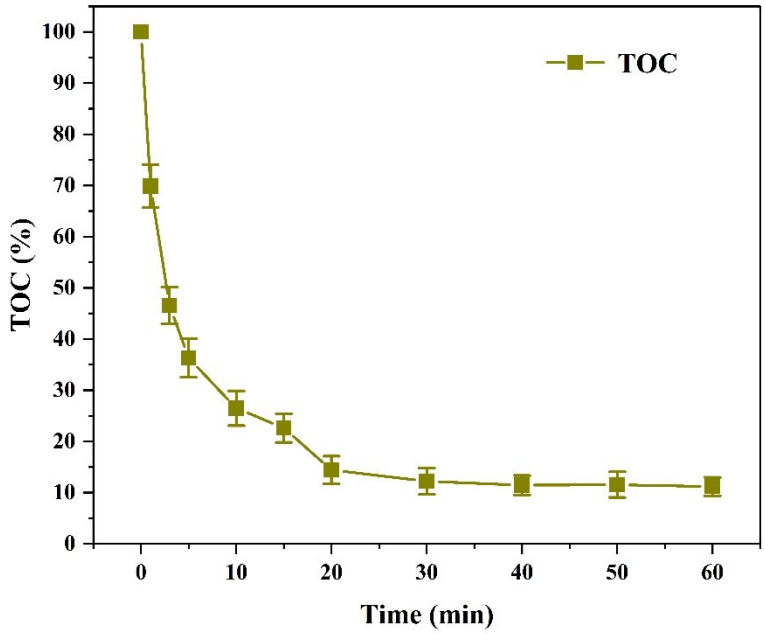


**Fig. S6. The decolorization of MB in terms of TOC removal (pH = 3.0, Temperature = 30℃, $C_{MB}$ = 20 mg $L^{-1}$, $V_{MB}$ = 30 ml, $m_{sample}$ = 30 mg, $V_{H2O2}/V_{MB}$=3%)**

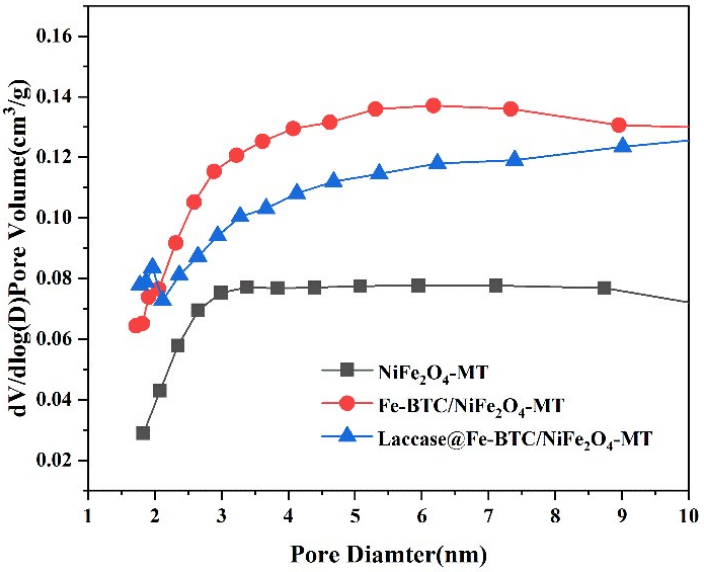


**Fig. S7. The pore distributions of samples (pore diameter between 2 nm and 10 nm).**

## Section 3: Tables

**Table. S1**. Pore texture parameters of the obtained samples

| Sample | $S_{BET}$ ($m^2g^{-1}$) | $S_{Micro}$ ($m^2g^{-1}$) | $V_{Total}$ ($cm^3g^{-1}$) | $V_{Micro}$ ($cm^3g^{-1}$) | $D_p$ (nm) |
|---|---|---|---|---|---|
| 1# | 45 | 0 | 0.117 | 0 | 10.5 |
| 2# | 121 | 9 | 0.277 | 0.004 | 9.19 |
| 3# | 160 | 48 | 0.309 | 0.027 | 7.73 |

[a] $S_{BET}$: BET specific surface area; $S_{Micro}$: micropore surface area; $V_{Total}$: total pore volume; $V_{Micro}$: micropore volume; $D_p$: average pore diameter. 1#: $NiFe_2O_4$-MT, 2#: Fe-BTC/$NiFe_2O_4$-MT, 3#: laccase@Fe-BTC/$NiFe_2O_4$-MT.

**Table. S2**. Movement rate, drag force and work efficiency of $NiFe_2O_4$-MT

| $H_2O_2$ /% | $v/10^{-6}$ m $s^{-1}$ | $F_{drag}/10^{-12}$ N | $P_{mecha}/10^{-15}$ W $motor^{-1}$ | $P_{chem}/10^{-8}$ W $motor^{-1}$ | $\eta/10^{-8}$ |
|---|---|---|---|---|---|
| 0.5% | 87.2±10.7 | 147±35.8 | 13.2±4.7 | 24.6±2.1 | 5.6±2.4 |
| 1% | 133.3±15.1 | 342.6±76.7 | 46.8±15.4 | 32.8±3.4 | 14.9±6.2 |
| 3% | 150±17.4 | 434±99.8 | 66.8±22.6 | 53.1±5.6 | 13.2±5.6 |
| 5% | 287.8±29.2 | 1592.7±320.1 | 467.8±138.7 | 114.5±11.2 | 42.4±16.3 |
| 10% | 1542.4±310.6 | 47103.1±18231.6 | 78313.6±42750.3 | 5577.5±512.3 | 148.7±90.3 |

**Table. S3**. Movement rate, drag force and work efficiency of laccase@Fe-BTC/$NiFe_2O_4$-MT

| $H_2O_2$ /% | $v/10^{-6}$ m $s^{-1}$ | $F_{drag}/10^{-12}$ N | $P_{mecha}/10^{-15}$ W $motor^{-1}$ | $P_{chem}/10^{-8}$ W $motor^{-1}$ | $\eta/10^{-8}$ |
|---|---|---|---|---|---|
| 0.5% | 71.7±9.7 | 99.5±26.3 | 7.4±2.9 | 8.1±0.6 | 9.4±4.2 |
| 1% | 125±12.3 | 300.2±58.3 | 38.2±11.0 | 55.8±6.9 | 7.2±2.9 |
| 3% | 141.7±16.5 | 387.1±88.8 | 56.3±18.9 | 51.0±5.4 | 11.6±4.9 |
| 5% | 300.0±27.5 | 1727.4±314.1 | 526.9±141.8 | 111.1±15.1 | 50.1±19.6 |
| 10% | 1316.7±278.3 | 34461.4±13943.1 | 49254.1±27947.7 | 1748.8±132.5 | 295.4±182.2 |

## Section 4

**The description of physical parameters**

The drag force, resistance and working efficiency of the $NiFe_2O_4$-MT and the laccase@Fe-BTC/$NiFe_2O_4$-MT were studied. It is assumed that the drag force generated by the bubble breaking away from the micromotor surface is equal to the steady-state fluid power. Therefore, the speed and force of the micromotor under low Reynolds coefficient can be estimated by the following formula:

$$F_{drag} = 6\pi\mu\gamma\upsilon \quad (1)$$

$v$ (m $s^{-1}$) is the speed of micromotor motion, $\mu$ (mPa s) is fluid viscosity, and $\gamma$ (m) is distance traveled in a given amount of time.

The kinetic energy of the micromotor driven by bubbles is actually converted from the chemical energy generated by the decomposition of $H_2O_2$ by $Mn_2O_3$. Therefore, the efficiency of the micromotor can be calculated by the following formula [1,2]:

$$\eta = P_{mecha} / P_{chem} \quad (2)$$

$$P_{mecha} = F_{drag} \cdot \upsilon = 6\pi\mu\gamma\upsilon^2 \quad (3)$$

$$P_{chem} = n \cdot \Delta r^{\theta} G \quad (4)$$

$$n = PV / RT \quad (5)$$

$$V = N \cdot 4\pi R_0^3 / 3 \quad (6)$$

$\eta$ is the efficiency of the micromotor, $P_{mecha}$ is micromotor mechanical power (W $motor^{-1}$), $P_{chem}$ is chemical input power (W $motor^{-1}$), which is equal to the chemical energy of all the gas produced, $V$ is the volume of an ideal gas. n is mol of gas (mol), $T$ is thermodynamic temperature of an ideal gas (K), $N$ is the number of bubbles per second, $R_o$ is the diameter of bubble (m) [3].

**Bradford analyses**

The Bradford method was used to determine laccase loading on Fe-BTC/$NiFe_2O_4$-MT by measuring of the initial and final concentrations of protein within the immobilization medium solutions. A calibration curve was plotted using Coomassie Brilliant Blue G-250 solutions as standards (0−24 mg/L). The laccase concentration in the solution can be determined with UV−vis spectrophotometry by measuring the absorbance at 595 nm. The amount of laccase immobilized onto Fe-BTC/$NiFe_2O_4$-MT was calculated by mass balance with the following equation:

$$\text{Laccase loading (mg/g)} = (C_0 - C_1)V/W_s \times 100\%$$

where $C_0$ is the initial laccase concentration (mg/mL), $C_1$ is the final laccase concentration (mg/mL),V is the laccase volume (mL), and $W_s$ is the support dose added (g) [4].

**Laccase leaching Test**

15 mg of laccase@Fe-BTC/$NiFe_2O_4$-MT ( was mixed with 3 mL of Acetic acid - sodium acetate buffer solution pH=3.0) and incubated at 4°C for different time, and then the solid fragment was removed. The protein concentration of the supernatant was determined by Bradford assay at different times as displayed in Fig.S5.

## References

1 W. Wang, T. Y. Chiang, D. Velegol and T. E. Mallouk, *Understanding the efficiency of autonomous nano-and microscale motors*, *J. Am. Chem. Soc.*, 2013, **135**, 10557-10565.

2 W. Gao, S. Sattayasamitsathit, J. Orozco and J. Wang, *Highly efficient catalytic microengines: template electrosynthesis of polyaniline/platinum microtubes*, *J. Am. Chem. Soc.*, 2011, **133**, 11862-11864.

3 B. J. Zhu, X. Y. Yu, Y. Jia, F. M. Peng, B. Sun, M. Y. Zhang, T. Luo, J. H. Liu and X. J. Huang, *Iron and 1,3,5-Benzenetricarboxylic Metal–Organic Coordination Polymers Prepared by Solvothermal Method and Their Application in Efficient As(V) Removal from Aqueous Solutions*, *J. Phys. Chem. C*, 2012, **116**, 8601-8607.

4 C. Chao, J. Liu, J. Wang, Y. Zhang, B. Zhang, and Y. Zhang, *Surface modification of halloysite nanotubes with dopamine for enzyme immobilization*, *Acs Applied Materials & Interfaces,* 2013, **5**, 10559-10564.